Influence of mobilized stem cells on myocardial infarct repair in a nonhuman primate model

Françoise Norol, Pascal Merlet, Richard Isnard, Pascale Sebillon, Nicolas Bonnet, Christian Cailliot, Claire Carrion, Maria Ribeiro, Frédéric Charlotte, Pascal Pradeau, Jean-François Mayol, André Peinnequin, Michel Drouet, Karima Safsafi, Jean-Paul Vernant, and Francis Herodin

Although previous findings have suggested that some adult stem cells are pluripotent and could differentiate in an appropriate microenvironment, the fate conversion of adult stem cells is currently being debated. Here, we studied the ability of mobilized stem cells to repair cardiac tissue injury in a nonhuman primate model of acute myocardial infarction. Mobilization was carried out with stem cell factor, 25 mcg/Kg/d (D), and granulocyte-colony-stimulating factor, 100 mcg/Kg/D administered 5 days before (D − 5 group; n = 3) or 4 hours after (H + 4 group; n = 4) circumflex coronary artery ligation; no growth factor was administered to 3 baboons of the control group. No adverse effect relating to growth factor administration was observed. Flk-1 and transcription factors of cardiac lineages could be detected in peripheral blood only by reverse transcriptase–polymerase chain reaction. When comparing positron emission tomography (PET) with [11C]-acetate between examinations from D2 and D30, a relative increase (perfusion ratio between infarct and noninfarct regions) of 26% (*P* = .01) in myocardial blood flow was found in the H + 4 group; the relative rate of oxidative metabolism remained unaltered in the 3 groups. No change was observed in the echographic indices of the left ventricular enlargement or systolic function in the 3 animal groups during the 2-month follow-up. The PET findings concurred with the immunohistochemistry analysis of left ventricular myocardial sections with evidence of endothelial cells but no myocyte differentiation; few cycling cells were observed at this time. Thus, the present data suggest that, in nonhuman primates submitted to coronary artery ligation, mobilization by hematopoietic growth factors could promote angiogenesis in the infarcted myocardium, without detectable myocardial repair. (Blood. 2003;102:4361-4368)

Introduction

Stem cells are undifferentiated cells, capable of proliferation and self-renewal and of producing large numbers of differentiated progeny. It was thought that only embryonic stem (ES) cells were pluripotent. Traditionally, the potential of adult stem cells for differentiation and tissue regeneration was considered to be restricted to the tissues in which they reside (multipotent cells). However, this view regarding adult stem cell potential recently has been challenged. Some findings suggest that stem cell biology may be more complex than originally anticipated; cells from somatic tissue could adopt hematopoietic fate,[1-3] and bone marrow hematopoietic cells could be turned into tissue.[4-6] Thus, some recent animal and clinical studies reported that, after myocardial infarction, bone marrow cells administered into the myocardium could induce a significant degree of tissue regeneration and functional improvement.[7,8] Orlic found that stem cell mobilization into peripheral blood could achieve similar results as a consequence of the formation of new myocytes, arterioles, and capillaries.[9] Migration of primitive cells via systemic circulation was suggested by the Anversa team, who found that human female hearts transplanted into male recipients showed a high level of chimerism, the presence of primitive hematopoietic cells, and differentiated cardiac cells of male origin.[10] Likewise, Korbling et al reported the donor origin of some hepatocytes and epithelial cells after allogeneic transplantation of mobilized hematopoietic stem cells.[11]

However, the pluripotentiality of adult hematopoietic stem cells has been challenged,[12,13] and the process of transdifferentiation, used to explain how tissue-specific cells can generate cells of other tissues, is debatable.[14,15] Thus, with regard to important theoretical and practical implications of the demonstration of adult stem cells, different in vitro and in vivo approaches should allow the previous data to be completed. A particularly attractive concept is that circulating stem cells are able to differentiate into specialized cells at distal sites, regardless of whether such cells originate from bone marrow or other tissues. Thus, we developed a nonhuman primate model of myocardial infarction and evaluated whether the administration of the stem cell factor (SCF) and granulocyte-colony stimulating factor (G-CSF) mobilized cells that were likely to help in myocardium repair.

From the Unité de Thérapie cellulaire, the Service de cardiologie, the Laboratoire de génétique et d'Insuffisance cardiaque (IFR14), the Service de Chirurgie cardiaque, the Inserm U523, the Laboratoire d'anatomopathologie, and the Service d'hématologie, GH Pitié Salpêtrière, Paris; Service de biophysique, CHU Mondor, Paris XII-AP-HP; Amgen France, Neuilly; Service Hospitalier Frédéric Joliot, CEA-DSV, Orsay; Institut de Médecine Aérospatiale du Service de Santé des Armées, Brétigny; and Centre de Recherches du Service de Santé des Armées, La Tronche, France.

Submitted March 5, 2003; accepted August 14, 2003. Prepublished online as *Blood* First Edition Paper, August 28, 2003; DOI 10.1182/blood-2003-03-0685.

Supported by grants from Amgen France, Association Française contre les Myopathies, Institut National de la Santé et de la Recherche Médicale, and Délégation Générale pour l'Armement.

Reprints: Francis Herodin, Centre de Recherches du Service de Santé des Armées, Departement of Radiobiology—Radiohematology Unit, 24 avenue des Maquis du Grésivaudan 38702—La Tronche Cedex France; e-mail: francis.herodin@wanadoo.fr.

The publication costs of this article were defrayed in part by page charge payment. Therefore, and solely to indicate this fact, this article is hereby marked "advertisement" in accordance with 18 U.S.C. section 1734.

Materials and methods

Animals and surgical procedure

The study was performed on adult male and female baboons having an average weight of 10 to 25 kg. Research was conducted in compliance with the principles of the French Army Ethics Committee on Animal Research. General anesthesia prior to surgery consisted of intramuscular ketamine (15 mg/kg), intravenous propofol (0.5 μg/kg), and intravenous sufentanil (0.5 μg/kg). All other invasive procedures and radiological examinations were carried out under general anesthesia with ketamine. On a daily basis, the animals received 1 mg/kg atenolol and 0.5 mg/kg aspirin orally.

Induction of myocardial infarction

The lateral branches of the circumflex coronary artery were ligated after short anterolateral thoracotomy in the fourth left intercostal space and after pericardiotomy. The pleural drain was removed before the animal was completely awakened. No revascularization was performed after infarct induction.

Stem cell mobilization

The mobilization protocol was based on previous primate studies.[16] Treated animals received subcutaneous injections of 2 hematopoietic growth factors, namely SCF (ancestim) 25 μg/kg and G-CSF (filgrastim) 100 μg/kg daily over a 12-day period. SCF and G-CSF administration started 5 days before infarct induction in 3 animals (group D − 5), and 4 hours after infarct induction in 4 animals (group H + 4). Three control animals received no growth factors. Full blood counts in treated and control animals were performed every 2 days until day 14. The G-CSF dose was reduced when the leukocyte count exceeded 70×10^9/L.

Characterization of cytokine-mobilized cells

Cytometric analysis. Enumeration of $CD34^+$ cells in peripheral blood (PB) was performed using a double-labeling with a phycoerythrin (PE)–conjugated anti–human CD34 monoclonal antibody (MoAb) (clone 566 BD Biosciences, Le Pont de Claix, France) and with fluorescein isothiocyanate (FITC)–conjugated anti-CD11b plus anti–CD2 MoAbs (no anti–human CD45 Ab is cross-reactive in baboons) followed by red blood cell lysis (Optilyse C, Beckman Coulter, Villepinte, France) shortly before cell analysis.

Identification of circulating cells was performed with PB-mobilized mononuclear cells (MNCs). MNCs were double-labeled as follows: (1) biotin-conjugated anti–CD34 MoAb (clone 566) and PE-conjugated anti-CD117 (BD Biosciences) with a second step with FITC-conjugated streptavidin (Dako Cytomation, Trappes, France); (2) unconjugated anti–VEGFR-2 (Flk1/KDR; Santa Cruz Biotechnology, Santa Cruz, CA) followed by FITC-conjugated rabbit anti–mouse Ab (Dako) as a secondary reagent and then implying a blocking step with unconjugated, nonspecific mouse IgG1 (Beckman Coulter) before using PE-conjugated anti–CD34 MoAb; (3) intracellular staining for GATA-2 and GATA-4 was performed by permeabilizing cells using a Cytofix Cytoperm kit (BD Biosciences) and incubating with PE-conjugated anti–CD34 MoAb and unconjugated mouse anti–GATA-2 MoAb or rabbit anti–GATA-4 polyclonal Ab (Santa Cruz Biotech). FITC-conjugated rabbit anti–mouse or goat anti–rabbit Ab (Sigma, Poole, United Kingdom) was used as a secondary reagent. Analysis was performed using an Epics XL flow cytometer (Beckman Coulter).

Reverse transcriptase–polymerase chain reaction (RT-PCR) for transcription factors. All primers used in this study were synthesized at Eurogentec (Saraing, Belgium) and designed with MacVector Software (Accelrys, Orsay, France). The forward (F) and reverse (R) primers selected are as follows: *GATA-2 F*: 5′ CAGACGACAACCACCACCTTATG 3′, R: 5′ CCTTCCTTCTTCATGGTCAGTGG 3′ generating a 119-bp DNA fragment; *Flk-1 F*: 5′ GTACCAGACCATGCTGGACTGC 3′, R: 5′ CTTGCAAGAGATTTCCCAAATG 3′ generating a 92-bp DNA fragment; *GATA-4 F*: 5′ TCAGAAGGCAGAGAGTGTGTCAA 3′, R: 5′ GATGCCGTTCATCTTGTGGTAGAG 3′ generating a 117-bp DNA fragment; *GATA-5 F*: 5′ CACAGACTTACGCACTTGTTTGGAC 3′, R: 5′ CCAGACAATTCATTCTGCCTGTCAG 3′ generating a 113-bp DNA fragment; *NFATC F*: 5′ TCTGGGAGATGGAAGCGAAAAC 3′, R: 5′ TTCCCGTTGCAGACGTAGAAAC 3′ generating a 130-bp DNA fragment; *Nkx2-5 F*: CAACAACAACTTCGTGAACTTCGG -3′, R: 5′ ATACCATGCAGCGTGGACACTC 3′ generating a 99-bp DNA fragment; *CYCA F*: 5′ CATCTGCACTGCCAAGACTGAGTG 3′, R: 5′ CTTCTTGCTGGTCTTGCCATTCC 3′ generating a 127-bp DNA fragment.

mRNA was isolated from 10^5 cells using a MagnNA Pure LC mRNA Isolation Kit I in a final volume of 30 μL (MagnaPure LC Instrument, Roche, Milan, Italy). Reverse transcription of mRNA was carried out in a final volume of 20 μL from 8 μL mRNA using a First Strand CDNA Synthesis kit with oligo (dT) according to the manufacturer's instruction (Roche Diagnostics, Mannheim, Germany).

The real-time PCR reaction was carried out with the LC Fast Start DNA Master SYBR Green kit (Roche Diagnostics) using 0.125 μL cDNA in a final volume of 20 μL, 4 mM MgCl2, and 0.4 μM for each primer (final concentration). Quantitative PCR was performed using Lightcycler (Roche Diagnostics) for 45 cycles at 95°C for 20 seconds, 58°C (CYCA, Flk-1, Nkx2.5) or 62°C (GATA, NFATC) for 5 seconds, and 72°C for 8 seconds.

Transcription factors and mRNA levels were expressed in relative copy numbers of target genes normalized against cyclophilin-A (CycA) mRNA. This was achieved by constructing a standard curve from a serially diluted (1 to 1000) positive control. Flk-1 mRNA expression could be detected after a number of cycles that reached the detection limit of RT-PCR. The experiment was repeated 3 times, the amplification specificity was controlled in each sample by fusion characteristics of the PCR product. For mRNA expressed at low levels, for instance, Flk-1 and Nkx2.5, a positive control was achieved using human umbilical vein endothelial cells (HUVECs) and baboon heart, respectively.

Comparative characterization of cells mobilized by SCF and G-CSF and by G-CSF alone. Similar cytometric and RT-PCR analysis were performed on mobilized MNCs from healthy human donors administered with G-CSF alone, after approval was obtained from the Groupe Hospitalier Pitie Salpetriere institutional review board for these studies, and informed consent was provided according to the Declaration of Helsinki. In the latter human MNCs, the CD133 expression was evaluated with PE-conjugated anti–human AC133 mAb (Miltenyi, Bergisch Gladbach, Germany).

Animal follow-up

Animals were studied using echocardiography and positron emission tomography (PET) with [^{11}C]-acetate. Echocardiography was performed 2 days prior to (D2), 2 days after (D2), 15 days after (D15), 30 days after (D30), and 60 days after (D60) myocardial infarct. Each animal underwent PET examination twice at D2 and D30 after coronary ligation.

Echocardiographic measurements. Echocardiography was performed in anesthetized animals using a Cypress echocardiograph (Acuson, Mountain View, CA) equipped with a high frequency transducer (7 Mhz). The anterior chest was shaved. A standard echocardiographic examination was performed in the left lateral supine position. 2-dimensional images were obtained in apical views in 2 orthogonal planes (4-chamber and 2-chamber apical views). End-diastolic and end-systolic areas (EDA and ESA) were measured in each plane at 3 different cardiac cycles. The average of 3 measurements was performed for each plane. The average of the values obtained in the 2-chamber and 4-chamber view was finally considered. The area ejection fraction was calculated as (EDA-ESA/EDA).

Positron emission tomography (PET) assessment of myocardial blood flow (MBF) and oxidative metabolism. Rationale: PET overcomes the physical limitations of previously available radionuclide imaging techniques (single photon computered tomography or SPECT) by providing the means for accurate attenuation correction, thus enabling absolute quantification of the concentration of radiolabeled tracer in the organ of interest. Attenuation is due to the fact that a fraction of the photons traveling through the body can be scattered by interactions with atomic electrons and can undergo change of direction and loss of energy: the apparent radioactivity measured is consequently less than the truth. Correction for attenuation is relatively straightforward in PET because of the mechanism of coincidence detection.

Absolute quantification of MBF, for instance, in mL/min/gram of tissue, has been achieved following the development of suitable tracer kinetic models. Oxygen-15–labeled water and nitrogen-13–labeled ammonia are the tracers most widely used for the quantification of regional MBF with PET, and they have been successfully validated in animals against the radiolabeled microsphere method. The potential for qualitative assessment of myocardial blood flow of [^{11}C]-acetate, which is a consequence of its high first-pass extraction, also has been validated by the close correlation found when comparing flow values obtained with both acetate and nitrogen-13–labeled ammonia.[17,18]

After acetate is extracted by the myocardial cell, 80% to 90% of it undergoes oxidation via the tricarboxylic acid cycle. The principal metabolite of acetate, CO_2, is cleared rapidly from the cell. Thus, when acetate is radiolabeled, the myocardial clearance of radiolabeled CO_2 directly reflects tricarboxylic acid cycle flux and oxidative metabolism. This correlates well with direct and indirect measurement of myocardial oxygen consumption in animal models and human. The contribution of other acetate metabolite pools in the cell to this rapid clearance is generally small, even with varying metabolic conditions and substrates.

Acquisition. PET with [^{11}C]-acetate assessment of blood flow and rate of oxidative metabolism was performed twice at D2 and D30 following the induction of an acute myocardial infarction.

PET was performed using an ECAT-953B/31 (CTI Siemens, Knoxville, TN), which collects 31 slices simultaneously, each with a thickness of 3.4 mm. The transverse and axial-intrinsic spatial resolutions are 6.0 mm and 4.8 mm, respectively. This scanner is equipped with 3-rod sources of [^{68}Ge] (approximately 300 MBq maximum total activity) to measure the attenuation coefficients (transmission scan during a 15-minute period).

After completion of the transmission scan, 358 ± 97 MBq of [^{11}C]-acetate was injected as a slow bolus over 30 seconds, and a dynamic emission sequence of 21 time frames over 30 minutes was acquired in 2D mode.

Data were reconstructed using the Filtered Back-Projection Algorithm (2DFBP) and a Hanning apodisation filter with a cutoff frequency of 0.5 cycles per pixel, without scatter correction.

Data analysis. The frames collected between 4.3 and 14 minutes after injection were summed, and the resulting image was used to visually draw several regions of interest (ROIs) over the left ventricular myocardium: the infarcted region (lateral wall), and noninfarcted, for instance, remote region (anteroseptal wall); an additional ROI was created in the midventricular-transaxial image plane to determine the blood pool used as an input function for myocardial blood flow (MBF) measurements. These regions were then applied to the corresponding images in the dynamic sequence, yielding myocardial and blood pool times versus activity curves.

From these curves, the K1 values were determined as previously described[17] for the noninfarcted (remote) and infarcted regions, using a one-tissue compartment model. MBF values were estimated as the K1 value (in mL/min/mL of myocardium) from 2 to 4 consecutive myocardial slices, depending on the heart size of each animal.

To estimate the rate of oxidative metabolism, a monoexponential function was fit to the myocardial time-activity data; the clearance rate constant (k-mono, in minute^{-1}) was determined as described previously.[18] The monoexponential fit begins at the point when the blood pool is stable (usually 2 to 4 minutes after the tracer injection). To minimize the influence of partial volume effect at the different PET examinations, K1 and k-mono values in the infarcted area were corrected with remote corresponding values (ratio of values measured in the infarcted area divided by those measured in the noninfarcted region).

Echocardiographic and PET analysis were performed by physicians (R.I., P.M., and M.R.) who were unaware of the therapeutic status of the animals.

Intrafibrosis cardiac tissue measurement

After the animals were killed, the hearts were harvested. A small sample of the infarcted and peri-infarcted area was cryopreserved; the hearts were then immediately set in 4% phosphate-buffered formalin. Each heart was transversely cut into 6-mm slices.

Five consecutive micrometer sections were prepared from different samples of the infarcted area. Paraffin-embedded sections were stained with hematoxylin/eosin; then, a digital acquisition of at least 10 sections was performed (XL objective) using the digital image analyzer software, LUCIA (Nikon, Tokyo, Japan), which performed a color analysis of each section, allowing the surface (μm^2) of fibrosis (slight pink) and of cardiac tissue included in fibrosis (dark pink) to be calculated. Then, the ratio between the surface of cardiac tissue and the total size of fibrosis was established.

Cell proliferation and differentiation

Paraffin-embedded sections were classically deparaffined and then heated in a microwave oven for 1 minute in a sodium citrate buffer (10 mM). After 2 washes with isotonic phosphate-buffered saline (PBS), some sections were blocked in 10% normal goat serum (NGS, Vector Laboratories, Burlingame, CA) in PBS for 1 hour at room temperature. They were then stained with antibodies against a cardiac myosin heavy chain (clone A4.1025; Alexis Biochemicals, Illkirch, France), Desmin (clone D33; Chemicon, Temecula, CA), connexin 43 and sarcomeric α-actin (Sigma) in order to evaluate the organization of myocytes. Endothelial cells were recognized by means of Ab anti-Flk1 (Santa Cruz Biotechnology) and anti–factor VIII (Dako). Hematopoietic cells were evaluated by staining with MoAb anti-CD34 and anti-CD90 (anti–Thy-1) (Pharmingen, San Diego, CA). Ki67 in nuclei was used to determine the proliferation status of the cells by using an anti–Ki67 MoAb (clone MIB-1). Immunohistochemistry labeling was followed by peroxidase reaction, using the LSAB 2 System HRP kit (Dako) according to the manufacturer's instructions. Double immunostaining was revealed by DAB-peroxidase reaction and Fastred-alkaline phosphatase reaction using Endovision (Dako). Analyses were performed with the microscope eclipse E800 (Nikon) with a 40 × or 60 × oil objective. Staining was evaluated on a semiquantitative scale (0-2+) by 3 blinded pathologists (P.S., C. Carrion, and F.C.).

Analysis of vessel numbers. To analyze the vessel density, 5 consecutive sections of infarcted area were randomly chosen; from each section, vessels were counted in the randomly chosen field of 500 μm^2.

Statistical analysis

All parameters were expressed as mean values ± standard deviation. Parameters were compared between the animal groups using a *t* test. Statistical significance level was set at 0.05.

Results

Fourteen animals were included in the study. One animal died during surgical procedure; 3 others died between D50 and D60 after infarct: one died from cardiac intractable ventricular arrhythmia, one died from sudden death with a large embolus found in the left ventricle at the autopsy, and one from a stroke. After these deaths, the following 10 animals received aspirin until they were killed, and no other complication was observed.

G-CSF and SCF induced no adverse effect despite myocardial infarct

No adverse reaction was observed during administration of SCF and G-CSF. In particular, the animals exhibited no complications involving a large number of circulating white blood cells, such as extensive cardiac complication or thrombosis events. Animal behavior was normal.

Mobilized cells contained cells of endothelial and cardiac lineage

CD34$^+$ cell mobilization. After administration of SCF and G-CSF, the circulating CD34$^+$ cells increased from day 3 and peaked between day 8 and day 12. The maximum number of CD34$^+$ cells in the peripheral blood had a mean of 73 ± 22/μL. In the control animals, the number of CD34$^+$ cells never exceeded 5/μL.

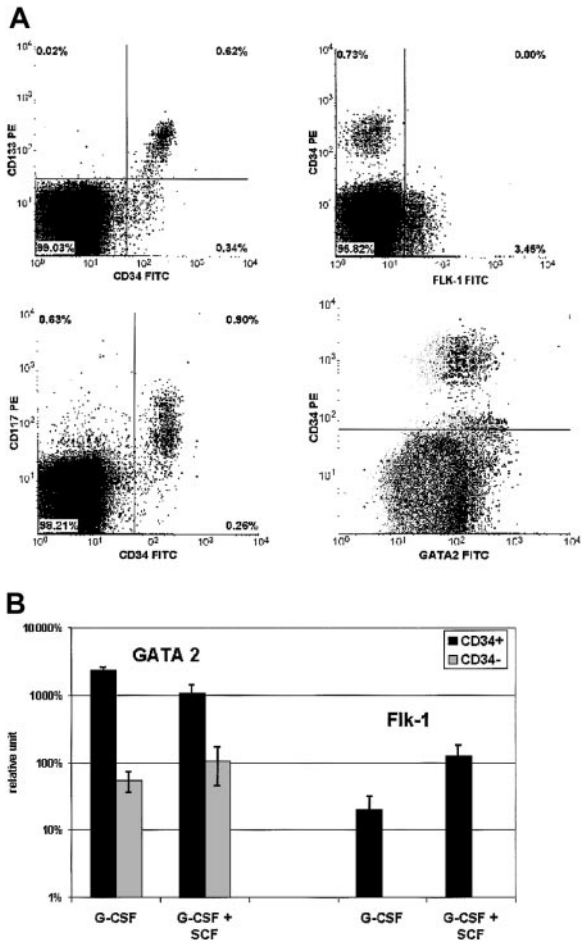

Figure 1. Endothelial cell mobilization. Cell markers of endothelial lineage were tested on PB MNCs of 4 baboons mobilized with G-CSF + SCF. Analysis could not be performed in animals not administered with cytokines, given the too-low number of $CD34^+$ cells in the circulation. Comparison was performed with mobilized MNCs from 6 healthy human donors administered with G-CSF alone. (A) Flow cytometric analysis: 4 biparametric dot plots show double-labeling with anti–CD133-PE MoAb and anti–CD34-FITC MoAb (top left), anti–CD117-PE MoAb and anti–CD34-FITC MoAb (bottom left), anti–CD34-PE MoAb and anti–FLK-1–FITC mAb (top right), anti–CD34-PE MoAb and anti–GATA2-FITC MoAb (bottom right), respectively. Bottom right dot plot displays overlapping negative control (gray dots, performed with anti–CD34-PE MoAb and nonspecific mouse MoAb) and positive test (black dots). The 3 other dot plots show positive tests. Results are representative of both baboon and human mobilized cell samples (except CD133/CD34 labeling, which can only be evaluated with human cells). (B) RT-PCR analysis: Analyzed samples are issued from baboons and healthy donors as indicated earlier in the legend for flow cytometric analysis. mRNA expression levels of GATA-2 and Flk-1 were analyzed by reverse transcription and real-time PCR. Transcription factors' mRNA levels, normalized against cyclophylin-A mRNA, are expressed as percentages of averaged mRNA levels of mobilized $CD34^-$ cells (error bars indicate standard deviation). Flk-1 mRNA was tested in $CD34^+$ cells and was detectable only at a low level, 50 to 100 times weaker than in HUVEC control cells.

Cell markers of endothelial and cardiac lineage were tested on circulating cells of baboons mobilized with SCF + G-CSF. Analysis could not be performed in the animals not administered with cytokines, given the too-low number of $CD34^+$ cells in peripheral blood. Comparison was performed with mobilized MNCs from healthy human donors administered with G-CSF alone.

Cytometry. As shown in Figure 1A, more than 65% of $CD34^+$ cells expressed CD117 and CD133. No $CD34^+$ cells were found to be Flk-1^+, but a small proportion of $CD34^-$ (from 0% to 5%) were Flk-1^+. With regard to intracellular GATA-2 expression, most $CD34^+$ cells coexpressed this transcription factor. A certain level of GATA-2 expression also was observed in part of the $CD34^-$ population. In contrast, no GATA-4 was observed in either subpopulation of mobilized cells. These markers were similarly expressed by G-CSF and G-CSF + SCF–mobilized MNCs (except for CD133, which can only be evaluated on human cells that were mobilized by G-CSF alone).

RT-PCR. In all growth factor–mobilized cell samples, GATA-2 (Figure 1B), GATA-4, and GATA-5 (Figure 2) were expressed much more in $CD34^+$ than $CD34^-$ cells. Thus, GATA-2 was 25-fold less expressed in $CD34^-$ cells, while GATA-4 and GATA-5 were observed only in $CD34^+$ cells as shown in Figure 2. GATA expression was higher in G-CSF samples than in G-CSF + SCF samples, especially with respect to GATA-5 ($P < .04$). The NAFTC expression was similar in $CD34^+$ and $CD34^-$ cells as presented in Figure 2. Flk-1 mRNA was detected at low levels in $CD34^+$ cells (Figure 1B), 50 to 100 times weaker than in HUVEC control cells. Nkx2.5 was detected only in 2 G-CSF $CD34^+$ cell samples and in one G-CSF + SCF $CD34^-$ cell sample, at a very low level. Using Nkx2.5 mRNA expression in baboon heart as a standard, the level in mobilized cells corresponds to about 1 positive cell in 100 $CD34^+$ cells.

Increase in myocardial blood flow for the infarcted area in some treated animals

When comparing the 3 animal groups at D2 PET examinations, there was no statistically significant difference for MBF (K1) or the rate of oxidative metabolism (k-mono) in the infarcted area and in the noninfarcted area.

When comparing PET myocardial blood flow at D2 and D30 after coronary ligation in each animal group, an increase in absolute myocardial blood flow was found for the infarcted area in treated animals, having received growth factors 4 hours after coronary ligation (from 0.43 ± 0.23 to 0.61 ± 0.26 mL/min/mL, $P < .01$); an increase in absolute myocardial blood flow was found in control animals for both infarcted areas and noninfarcted (remote) regions (from 0.45 ± 0.18 to 0.61 ± 0.26 mL/min/mL, and from 1.03 ± 0.09 to 1.44 ± 0.61 mL/min/mL, respectively, $P < .05$). When considering the relative change (ratio of values in infarcted regions compared with those in remote regions) in myocardial blood flow, a 26% increase between D2 and D30 examinations was found in the H + 4 group (from 0.39 ± 0.17 to

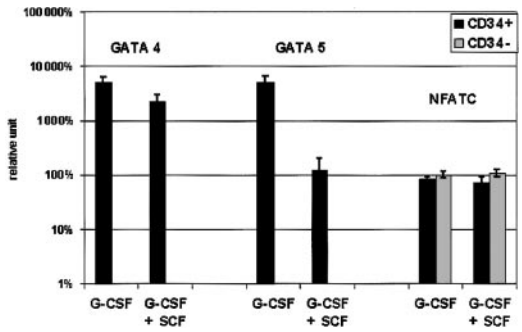

Figure 2. Cardiac cell mobilization. RT-PCR analysis. Samples are issued from MNCs mobilized by G-CSF + SCF in baboons and G-CSF alone in healthy human donors as described in Figure 1. mRNA expression levels of GATA-4, GATA-5, and NFATC were analyzed by reverse transcription and real-time PCR. Transcription factors' mRNA levels, normalized against cyclophylin-A mRNA, are expressed as percentages of averaged mRNA levels of mobilized $CD34^-$ cells (error bars indicate standard deviation). Nkx2.5 was detected only in 2 G-CSF–mobilized $CD34^+$ cell samples and in one G-CSF + SCF $CD34^-$ cell sample, at a very low level.

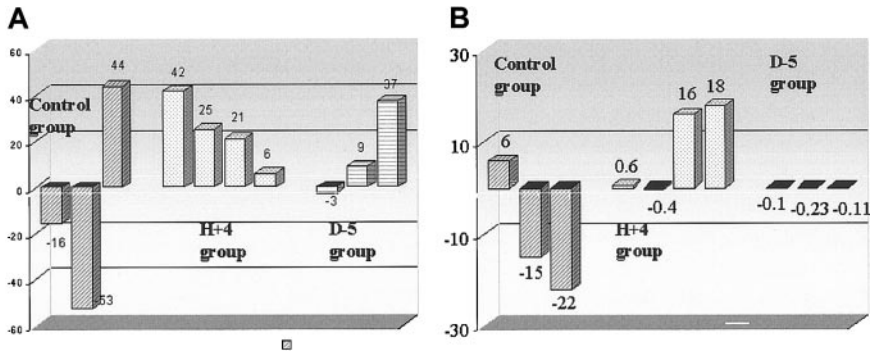

Figure 3. Cardiac blood flow and metabolism. Histograms indicate the recovery of (A) myocardial blood flow (rMBF in mL/min/mL of myocardium) and (B) oxygen production (oxidative metabolism, k-mono, in minute^{-1} of myocardium) in infarcted areas after 1 month of follow-up, in treated animals, mobilized 5 days before (D − 5) or 4 hours after (H + 4) ligation, and in control animals; as indicated in "Materials and methods," so as to account for hemodynamic differences at the different PET examinations, values in the infarcted area were corrected with noninfarcted (remote) area values. Then, the ratios up to 2 days after coronary ligation were calculated.

0.50 ± 0.14, $P < .01$), while no changes were observed in the 2 other groups (Figure 3).

When comparing the PET oxidative metabolism at D2 and D30 after coronary ligation in each animal group, an increase was found in H + 4 animals for both the infarcted area and noninfarcted (remote) regions (from 0.065 ± 0.017 to 0.093 ± 0.016 minutes^{-1} and from 0.091 ± 0.009 to 0.118 ± 0.009 minutes^{-1}, respectively, $P < .05$). But, when considering the relative change (ratio of values in infarcted regions compared with those in remote regions), no difference in the rate of oxidative metabolism was observed within the 3 animal groups between D2 and D30 examinations. Figure 4 shows a representative PET examination.

Myocardial function was not improved by growth factor administration

The effects of growth factor administration on myocardial remodeling and systolic function were evaluated by echocardiography (Figure 5). Before coronary ligation, the ejection systolic area (ESA) and the left ventricular ejection fraction (LVEF) were, respectively, 5.4 ± 1.0 cm^2 and 51.2% ± 1.9% in the treated group and 5.3 ± 0.9 cm^2 and 49.5% ± 5.3% in the control group. After coronary ligation, treated baboons exhibited larger infarcts: thus, ESA had an increase, on average, of 49% and 28% in the treated and control animals, respectively, while EF had a decrease of 29% in treated animals and 13.8% in control animals.

Measurement of LVEF during the follow-up period showed no improvement of cardiac performance in treated animals compared with control animals (Figure 5A). In treated animals, the LVEF decreased at D15, whereas it slightly improved at D30 and D60 by 2.2% ± 0.9% and 7% ± 2.1%, respectively, compared with the postmyocardial infarction value; in control animals, the recoveries at D30 and D60 were, respectively, 8.5% and 8.9%. There was also no attenuation in cavitary dilation (Figure 5B). Two weeks after infarction, in treated and control animals, a further increase in the left ventricular volume was found. At 1 month, the ESA continued to slightly increase (5.7% ± 1.3%) in treated animals, while it showed a slight improvement of 10.5% ± 5.1% in control animals. At 2 months, the ESA improved only by 3.08% ± 1.37% in treated animals and by 10.3% ± 6.1% in control animals. Diastolic areas also remained unchanged during the follow-up (Figure 5C).

Overall, there was no significant difference between control and treated animals at day 15, 30, or 60 after myocardial infarction and after 2 months after infarction; growth factor administration did not attenuate the left ventricle dilation nor did it improve contractile performance.

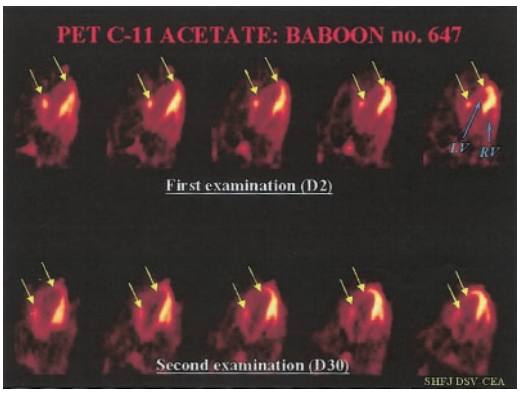

Figure 4. Representative PET examination. Ten-minute static PET myocardial images obtained 6 minutes after injection of C-11 acetate in a treated baboon. Each time, we can compare 5 consecutive transverse myocardial slices from the top (2 days after coronary artery ligation) to the bottom (30 days after myocardial infarction) of the heart: (LF) = left ventricle, (RV) = right ventricle. At day 2, we can see a large, nonviable antero-lateral myocardial infarction (between the 2 arrows in yellow). The mean value of myocardial blood flow decreased in the infarcted area (0.28 mL/min/g of tissue versus 0.75 mL/min/g of tissue in the remote, noninfarcted areas). At day 30, there was a slight increase in tracer uptake in the center of the necrotic zone, but also a clear increase in tracer uptake in the peripheral regions of the necrotic lesion, which led to a reduction of the infarct size (indicated by yellow arrows). At this time, MBF was 0.71 mL/min/g of tissue in the necrotic area versus 0.88 mL/min/g of tissue in the remote areas.

Growth factor administration induced endothelial cell but not other specialized cardiac cell differentiation

Ki67 was assayed to determine whether there were cycling cells at the time of death. The Ki67 expression was found in only a few section examinations in 2 treated animals. According to the semiquantitative scale evaluation, there was no difference between treated and control animals in proliferating cells at this time (Figure 6D-F).

Factor VIII labeling showed the regeneration of vascular structures in treated animals. Vessels with a luminal diameter of 12 to 100 micrometers or larger with a diameter more than 100 micrometers were detected in all but one treated animal (Figure 6A-C); Flk-1–positive cells, and other endothelial cell markers, were also present in the infarcted area in this group. Double immunostaining showed that cycling cells expressed Factor VIII (Figure 6F). The total number of vessels evaluated in randomly chosen areas statistically increased ($P < .01$) with a 2.3-fold increment in treated versus control animals.

Four cytoplasmic proteins were used to identify differentiated myocytes: cardiac myosin, desmin, sarcomeric-actin, and connexin 43. In healthy myocardium, cardiac fibers are a system of thick and thin interdigitating filaments, characterized by the organization of the contractile proteins into striated myofibrils, which result from repeating units arranged in series or sarcomeres (Figure 6G). In

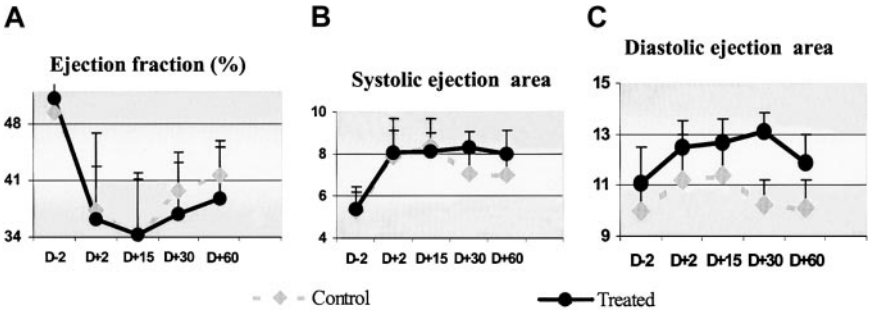

Figure 5. Cardiac anatomy and function. The effect of SCF and G-CSF mobilization on the (A) ejection fraction, and cavitary dilation (B) in systole and (C) diastole over a 2-month period before and after circumflex artery ligation: control animals (n = 3); treated animals (n = 7). Values are mean ± SD. Administration of growth factors induced no significant improvement of these parameters.

some sections of the infarcted area, cardiac myosin and desmin were expressed for both treated and control animals; but, as shown in Figure 6H-I, compared with healthy myocardium, a disorganization of cardiac sarcomeres was observed. No expression of sarcomeric-actin and connexin 43 was detected. These observations provided little evidence for newly forming myocardium but were more consistent with residual cardiac myocytes in fibrosis.

We also determined if circulating hematopoietic cells could be detected in the myocardium at this time; an antibody against the largely expressed hematopoietic protein, CD45, is not available in baboons; however, we looked for the expression of CD34 antigen and Thy-1 (CD90), which identifies more primitive hematopoietic cells. No staining of the hematopoietic cell marker was observed.

Similar patterns of fibrosis in both treated and untreated animals

We determined, after hematoxylin/eosin coloration and use of a digital color image analysis, that the area of myocardial tissue included in fibrosis did not increase in animals having received growth factors; the ratio between the cardiac tissue surface and the total size of fibrosis (μm^2) was similar in treated and in control animals, 0.23 and 0.19, respectively. As shown in Figure 7, there was a similar scar aspect composed of a dense, fibrous paucicellular tissue. This cardiac tissue could probably be related to residual cardiac cells rather than regenerating myocytes.

Discussion

After a heart attack, recovery of the myocardium is limited by its inability to regenerate and by inadequate revascularization of the viable ventricular tissue. Current clinical interventions are usually not sufficient to prevent left ventricular remodeling and the subsequent development of heart failure, underscoring the need for more efficient therapies. One approach focuses on the repopulation of injured myocardium by transplantation of healthy cells such as fibroblasts, skeletal myoblasts, primary myocardial cell cultures, cardiomyocytes derived from stromal cells, and, more recently, bone marrow cells.[19-21] These trials involved the implementation of cells directly into the myocardium. Recent findings suggest that stem cells mobilized in peripheral blood could provide differentiation of specialized cells at distal sites and offer a more suitable therapeutic answer for many kinds of injured tissues.

Thus, the present study was designed to determine, in a nonhuman primate model of acute myocardial infarction, whether putative pluripotent stem cells could be mobilized by administering hematopoietic growth factors after injury to restore damaged

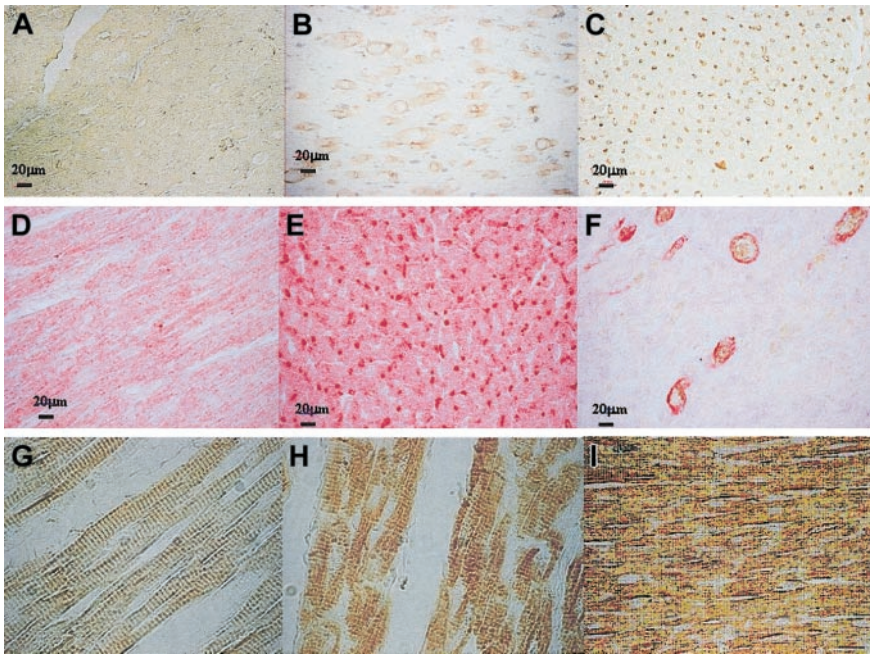

Figure 6. Markers of proliferation and of differentiating cardiac cells. (A-C) Immunophenotypic characterization of cells of endothelial lineage demonstrated in treated animals versus control animals (A), diffuse increase in capillaries (B) > 100 micrometer diameter or (C) of 12 to 100 micrometers; (D-F) double immunostaining showed that cycling Ki67$^+$ cells expressed FVIII (Ki67 appeared in brown and was revealed by DAB-peroxidase reaction and FVIII appeared in red and was revealed by Fastred–alkaline phosphatase reaction) (F), most of endothelial lineage cells did not express Ki67 (E), control animals (D). (G-I) In the healthy myocardium, cardiac myocytes are characterized by the organization of the contractile proteins into striated myofibrils, resulting from repeating units arranged in series, the sarcomeres (G). Myosin was expressed in some sections of the infarcted area, but a disorganization of cardiac sarcomeres was observed in treated animals (H) as well as in control animals (I). Original magnifications: A-F, × 40; G-I, × 60.

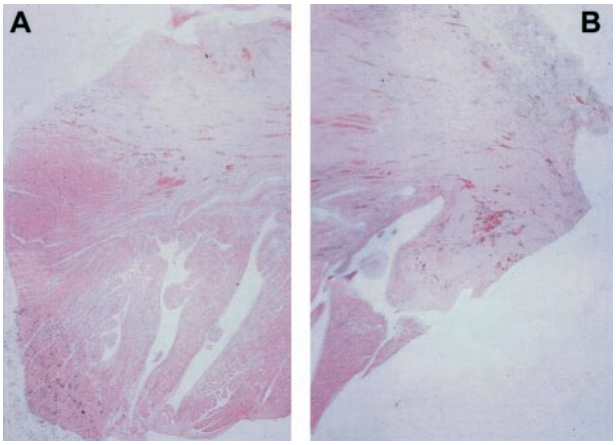

Figure 7. Evaluation of cardiac tissue in fibrosis in infarct zone. Two months after coronary artery ligation, staining with hematoxylin/eosin demonstrated in animals (A) that received or (B) did not receive growth factors similar scar aspects composed of paucicellular, dense, fibrous tissue; the digital image analyzer software, LUCIA, allowed a similar ratio of cardiac tissue (dark pink) included in fibrosis (slight pink) to be calculated.

tissues. The data indicate that the mobilizing treatment induced the regeneration of vascular structures in treated animals with a significant increase in the total numbers of capillaries and arterioles, when compared with control animals. A significant improvement in remaining myocardial blood flow was found in vivo using PET during the first month after acute myocardial infarction in the animal group treated with hematopoietic growth factors 4 hours after injury. Endothelial cells, defined by the expression of the vascular endothelial growth factor (VEGF) receptor (Flk-1) in the $CD34^+$ cell population, could be detected in peripheral blood after mobilization only by RT-PCR; in order to identify human, adult bone marrow (BM)–derived angioblast, as proposed by Kocher et al,[22] some cellular RNA and protein expression of the transcription factor GATA-2 was found in the $CD34^+$ cell population. Nevertheless, we cannot eliminate the possibility that the regeneration of vascular structures could come from resident cardiac stem cells or that it could possibly be a direct influence of growth factors on local heart vascularization. Thus, it was recently demonstrated that G-CSF could promote, in a murine model, an accelerated tumor growth associated with enhancement of neovascularization in the tumor and enhance vascular graft endothelialization from circulating blood cells.[23] The importance of BM-derived endothelial precursors in the restoration of myocardial revascularization after infarction also was suggested in 2 other animal studies. Using human donors and athymic rat recipients, a significant increase in revascularization of postinfarction myocardial tissue was achieved by the intravenous administration of cytokine-mobilized BM-derived angioblast.[22] Development of neovascularization was also reported after the implantation of BM MNCs into an ischemic myocardium of swine with the enhancement of collateral perfusion, related to the ability of BM cells to secrete potent angiogenic ligands and cytokines such as VEGF and basic fibroblast growth factor (FGF).[24] Finally, similar effects of BM cells were suggested in 2 preliminary clinical trials.[8,21] However, we did not observe new myocyte development, which is in contrast with the previous observation by Orlic et al in a murine model.[9] This correlated with the lack of reduction in myocardial remodeling and improvement of ventricular function after administering growth factors. Three hypotheses could be raised: (1) true adult stem cells exist in mice but disappear in higher species; (2) we could not observe myocyte differentiation since the time required to develop from the stem cells went beyond the 2-month follow-up; late improvement of the function associated with perfusion improvement up to 7 months as opposed to 5 weeks has been reported in patients after myocardial infarction.[25] Nevertheless, the low level of cell proliferation measured by the expression of Ki67 does not seem to support later differentiation; and finally, (3) the nature and number of the mobilized cells may differ in mice and primates. The combination of the hematopoietic growth factors used may have limited ability to mobilize pluripotent cells in primates; mobilized pluripotent cells may have limited ability to specifically reach and be concentrated in the injured tissues. In this way, our study design did not include the reopening of the coronary artery after the infarct was induced so as to exclusively measure the specific effects of mobilization; repair could only be obtained from the developing cells in the paranecrotic area. Greater efficiency could be achieved with a reperfusion of the infarcted area, as it is usually performed in clinical settings. Thus, our data indicate that several cardiomyocyte transcription factors have been identified in mobilized mononuclear circulating cells and have shown to be predominant in $CD34^+$ cells. The zinc finger proteins, GATA4 and GATA5, NFATC, and Nkx2.5 have been shown to be required for various stages of cardiomyocyte development, endocardial differentiation, and heart morphogenesis.[26] These transcription factors could be detected at variable levels by RT-PCR and were similarly represented in mononuclear cells mobilized by the combination of SCF and G-CSF used in our nonhuman primate model or by G-CSF alone, administered to healthy donors; given this, G-CSF has minor side effects compared with SCF and will be more suitable for clinical application than a combination of G-CSF and SCF, which was initially proposed based on the ability of this combination to mobilize more primitive progenitors than G-CSF alone.[27] Nevertheless, the value of these transcription factors as predictive of the mobilization of cardiac progenitors remains to be confirmed; particularly, Nkx2.5, the most specific one,[28] was detected in only 3 samples.

The approach that involves the use of cells transduced with a lentiviral vector will make it possible to address these questions. The benefit of a lentiviral vector is that it allows efficient transduction of quiescent or slightly activated cells. However, this approach is limited in its ability to effectively transduce the "true" stem cells.

In conclusion, our study demonstrates that cardiac neovascularization could be developed after administering growth factors, probably related to the mobilization of endothelial precursors. The functional value of this neovascularization and the ability of mobilized cells to induce therapeutic angiogenesis of ischemic tissues still remain to be confirmed.

Acknowledgments

We are grateful to Dr G. Brunetti for help with echocardiography, Dr G. Uzan for providing endothelial cells and Flk-1 primers, and Dr J. T. Vilquin for discussions. We are indebted to D. Lici, C. Boismon, and S. Gouard for their technical assistance. We thank Amgen (Thousand Oaks, CA) for providing G-CSF and SCF, and anatomopathology laboratory technicians for slice preparations.

References

1. Clarke DL, Johansson CB, Wilbertz J, et al. Generalized potential of adult neural stem cells. Science. 2000;288:1660-1663.
2. Jackson KA, Mi T, Goodell MA. Hematopoetic potential of stem cells isolated from murine skeletal muscle. Proc Natl Acad Sci U S A. 1999;96: 14193-14195.
3. Gussoni E, Soneoka Y, Strickland CD, et al. Dystrophin expression in the mdx mouse restored by stem cell transplantation. Nature. 1999;401:390-394.
4. Brazelton TR, Rossi FM, Keshet GI, Blau HM. From marrow to brain: expression of neuronal phenotypes in adult mice. Science. 2000;290: 1775-1779.
5. Mezey E, Chandross KJ, Harta G, Maki RA, McKercher SR. Turning blood into brain: cells bearing neuronal antigens generated in vivo from bone marrow. Science. 2000;290:1779-1782.
6. Lagasse E, Connors H, Al-Dhalimy M, et al. Purified hematopoietic stem cells can differentiate into hepatocytes in vivo. Nat Med. 2000;6: 1229-1234.
7. Orlic D, Kajstura J, Chimenti S, et al. Bone marrow cells regenerate infarcted myocardium. Nature. 2001;10:701-705.
8. Stamm C, Westphal B, Kleine HD, et al. Autologous bone-marrow stem-cell transplantation for myocardial regeneration. Lancet. 2003;361: 45-46.
9. Orlic D, Kajstura J, Chimenti S, et al. Mobilized bone marrow cells repair the infarcted heart, improving function and survival. Proc Natl Acad Sci U S A. 2001;98:10344-10349.
10. Quaini F, Urbanek K, Beltrami AP, et al. Chimerism of the transplanted heart. N Engl J Med. 2002;346:5-15.
11. Korbling M, Katz LR, Khanna A, et al. Hepatocytes and epithelial cells of donor origin in recipients of peripheral-blood stem cells. N Engl J Med. 2002;346:738-746.
12. Holden C, Vogel G. Plasticity: time for a reappraisal. Science. 2002;296:2126-2129.
13. Wagers AJ, Sherwood RI, Christensen JL, Weissman IL. Little evidence for developmental plasticity of adult hematopoietic stem cells. Science. 2002;297:2256-2259.
14. Qi-Hong Ying, Nichols J, Evans EP, Smith AG. Changing potency by spontaneous fusion. Nature. 2002;416:545-547.
15. Terada N, Hamazaki T, Oka M, Hoki M, et al. Bone marrow cells adopt the phenotype of other cells by spontaneous cell fusion. Nature. 2002; 416:542-545.
16. Andrews RG, Briddell RA, Knitter GH, et al. In vivo synergy between recombinant human stem cell factor and recombinant human granulocyte colony-stimulating factor in baboons enhanced circulation of progenitor cells. Blood. 1994;84: 800-810.
17. van den Hoff J, Burchert W, Borner AR, et al. [1-(11)C] Acetate as a quantitative perfusion tracer in myocardial PET. J Nucl Med. 2001;42: 1174-1182.
18. Sun KT, Yeatman A, Buxton DB, et al. Simultaneous measurement of myocardial oxygen consumption and blood flow using [1-carbon-11] acetate. J Nucl Med. 1998;39:272-280.
19. Wang JS, Shum-Tim D, Galipeau J, Chedrawy E, Eliopoulos N, Chiu RC. Marrow stromal cells for cellular cardiomyoplasty: feasibility and potential clinical advantages. J Thorac Cardiovasc Surg. 2000;120:999-1005.
20. Menasche P, Hagege AA, Scorsin M, et al. Myoblast transplantation for heart failure. Lancet. 2001;357:279-280.
21. Assmus B, Schachinger V, Teupe C, et al. Transplantation of progenitor cells and regeneration enhancement in acute myocardial infarction. Circulation. 2002;106:3009-3017.
22. Kocher AA, Schuster MD, Szabolcs S, et al. Neovascularization of ischemic myocardium by human bone marrow–derived angioblasts prevents cardiomyocyte apoptosis, reduces remodeling and improves cardiac function. Nat Med. 2001;7: 430-436.
23. Shi Q, Bhattacharya V, Hong-De Wu M, Sauvage LR. Utilizing granulocyte colony-stimulating factor to enhance vascular graft endothelialization from circulating blood cells. Blood. 2000;95:952-958.
24. Kamihata H, Mastsubara H, Nishiue T, et al. Implantation of bone marrow mononuclear cells into ischemic myocardium enhances collateral perfusion and angiogenic ligands and cytokines. Circulation. 2001;104:1046-1052.
25. Galli M, Marcassa C, Bolli R, et al. Spontaneous delayed recovery of perfusion and contraction after the first 5 weeks after anterior infarction: evidence for the presence of hibernating myocardium in the infarcted area. Circulation. 1994;90: 1386-1397.
26. Nemer G, Nemer M. Cooperative interaction between gata5 and NF-ATc regulates endothelial-endococardial differentiation of cardiogenic cells. Development. 2002;129:4045-4055.
27. Hess DA, Levac KD, Karanu FN, et al. Functional analysis of human hematopoietic repopulating cells mobilized with granulocyte colony-stimulating factor alone versus granulocyte colony-stimulating factor in combination with stem cell factor. Blood. 2002;100:869-878.
28. Shirai M, Osugi T, Koga H, et al. The Polycomb-group gene Rae28 sustains Nkx2.5/Csx expression and is essential for cardiac morphogenesis. J Clin Invest. 2002;110:177-184.